NANO LETTERS

pubs.acs.org/NanoLett Letter

CRISPR-Cas12a-Based Nucleic Acid Amplification-Free DNA Biosensor via Au Nanoparticle-Assisted Metal-Enhanced Fluorescence and Colorimetric Analysis

Jin-Ha Choi,[§] Joungpyo Lim,[§] Minkyu Shin, Se-Hwan Paek,* and Jeong-Woo Choi*

Cite This: https://dx.doi.org/10.1021/acs.nanolett.0c04303 Read Online

ABSTRACT: Cell-free DNA (cfDNA) has attracted significant attention due to its high potential to diagnose diseases, such as cancer. Still, its detection by amplification method has limitations because of false-positive signals and difficulty in designing target-specific primers. CRISPR-Cas-based fluorescent biosensors have been developed but also need the amplification step for the detection. In this study, for the first time CRISPR-Cas12a based nucleic acid amplification-free fluorescent biosensor was developed to detect cfDNA by a metal-enhanced fluorescence (MEF) using DNA-functionalized Au nanoparticle (AuNP). Upon activating the CRISPR-Cas12a complex by the target cfDNA and subsequent single-strand DNA (ssDNA) degradation between AuNP and fluorophore, MEF occurred with color changes from purple to red-purple. Using this system, breast cancer gene-1 (BRCA-1) can be detected with very high sensitivity in 30 min. This rapid and highly selective sensor can be applied to measure other nucleic acid biomarkers such as viral DNA in field-deployable and point-of-care testing (POCT) platform.

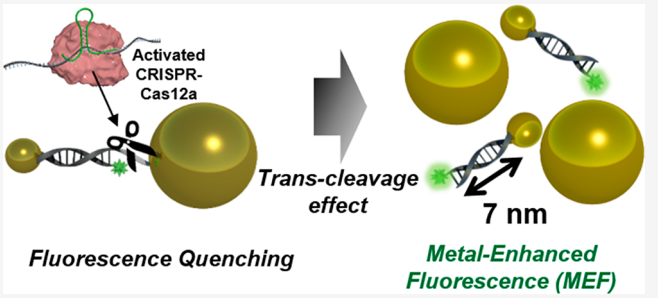

KEYWORDS: *CRISPR-Cas12a, Metal-enhanced fluorescence (MEF), Cell-free DNA (cfDNA), Colorimetric analysis, Au nanoparticle*

Clustered regularly interspaced short palindromic repeats (CRISPR) systems provide adaptive immunity to bacteria to degrade intruding nucleic acids. These systems have been utilized as gene-editing tools due to their ability to recognize and degrade target nucleic acid sequences after the Cas protein scans and identifies the target nucleic acid sequence through the direction of a guide RNA.[1−4] Because of these properties, the CRISPR-Cas system is actively applied in diverse biomedical fields such as gene delivery, cancer therapy, stem cell engineering, pharmacology, and biosensors.[5−14] Within the CRISPR-Cas family, CRISPR-Cas12a is known to possess a unique trans-cleavage effect (collateral effect), which allows for indiscriminate cleavage of ambient single-stranded DNA (ssDNA) when activated by a matching target DNA.[15−17] Recently, these properties have been widely applied to the development of novel biosensing techniques to measure the fluorescence intensity generated when the target DNA-binging CRISPR-Cas12a complex is degraded to ssDNA (connected to a fluorophore and quencher) randomly via the aforementioned trans-cleavage effect.[18−20] In order to improve the sensitivity of target DNA detection, nucleic acid amplification techniques, such as loop-mediated isothermal amplification (LAMP) and recombinase polymerase amplification (RPA), are implemented to the CRISPR-Cas12a-based biosensor. For example, the human papillomavirus (HPV) DNA was amplified via RPA for rapid, simple, and sensitive detection of CRISPR-Cas12a assisted biosensor.[18] However, nucleic acid amplification entails some notable disadvantages. Particularly, this approach could induce false-positive results and requires specialized experimental equipment as well as many reagents such as nucleotide mix, target DNA primers, and reverse transcriptase. Furthermore, the process is difficult to design target-specific primer, time-consuming, costly, and requires skilled technicians to perform the analysis.[19−21]

Cell-free DNA (cfDNA) is derived from apoptosis, necrosis, and active release from cancer cells, and it is recognized at a high level in advanced cancer or patients with early stage disease.[22] Therefore, the measurement of cfDNA is a significant early diagnostic strategy to ensure rapid treatment, thereby elevating the chances for full recovery. In addition, cfDNA is an attractive and minimally invasive biomarker and an alternative to tissue biopsy for the diagnosis of diseases and mutations.[23] Despite the high potential, cfDNA is not yet widely implemented in the clinic due to its low abundance in blood and other bodily fluids.

Received: October 27, 2020
Revised: December 16, 2020

Noble metal nanomaterials (NMNs) have inherent surface plasmon resonance (SPR) property, which is defined as the oscillating movement of electromagnetic waves that propagate in parallel along with a noble metal/dielectric interface.[24,25] This property can be used in various ways to enhance the primary signal intensity. For example, there are many cases where biomaterials are detected by surface-enhanced Raman spectroscopy (SERS) or metal-enhanced fluorescence (MEF) signals with NMNs such as Au and Ag nanomaterials.[26−28] In the case of MEF, NMNs paradoxically also function as fluorescence quenching agents when the distance between the fluorophore and NMNs is below approximately 2 nm.[27,29,30] Therefore, if NMNs are paired with the CRISPR-Cas system, it is possible to easily maximize the difference of the intensity between the target-negative and target-positive and improve the sensitivity without any nucleic acid amplification step. However, no previous CRISPR-Cas based detection systems by MEF have reported such an approach yet.

To this end, in this study CRISPR-Cas12a-based cfDNA biosensing system by Au nanoparticle (AuNP)-assisted MEF was developed without the nucleic acid amplification process. Currently, we have already studied MEF-based intracellular caspase-3 biosensor for the sensitive detection of preapoptotic cells by MEF using 60 nm sized AuNPs.[31] In the present study, two different-sized AuNPs (20 and 60 nm) pairs connected by a 7 nm long double-strand DNA (dsDNA) and a 2 nm long ssDNA were introduced to induce MEF with target DNA and fluorescence quenching without target DNA. Fluorescein isothiocyanate (FITC) was bound to one of the ends of the dsDNA that was not connected to the 60 nm sized AuNPs (60-AuNPs) and remained in a quenching state due to its proximity to the 60-AuNPs. However, if target cfDNA is present, the ssDNA between the 20- and 60-AuNPs was cleaved by the activated CRISPR-Cas12a complex, which resulted in the dissociation of the 60-AuNPs from FITC with the 7 nm long DNA functionalized 20-AuNPs, thereby inducing a fluorescence signal that was proportional to the target cfDNA concentration down to femtomolar concentration ranges without the need for nucleic acid amplification. In addition, given that the wavelength of the absorbance peaks varied depending on the size and distance of each AuNP, the cfDNA concentration could also be inferred through colorimetric analysis within a nanomolar scale precision. In summary, the implementation of MEF greatly improved the sensitivity of cfDNA detection, which resulted in femtomolar detection of the BRCA-1 gene, a representative cfDNA closely related to breast cancer.

RESULTS AND DISCUSSION

Characterization of DNA-Functionalized AuNPs for cfDNA Detection by CRISPR-Cas12a. During the CRISPR-Cas12a-mediated trans-cleavage reaction, ambient ssDNA must be degraded by the target-bound CRISPR-Cas12a complex (activated CRISPR-Cas12a), whereas dsDNA cannot be cleaved. On the basis of this particular phenomenon, a DNA-functionalized AuNP nanosensor was designed for the induction of quenching and MEF (Figure 1). Specifically, 20-AuNP was functionalized to an approximately 7 nm long FITC-tagged ssDNA. This DNA-functionalized 20-AuNP played a crucial role as a fluorescence signal enhancer by contributing MEF. Additionally, a 60-AuNP was also functionalized to the ssDNA, which could bind to the ssDNA on the 20-AuNPs via complementary binding. This 60-AuNP complex hampered the fluorescence signal generation of FITC, effectively acting as a

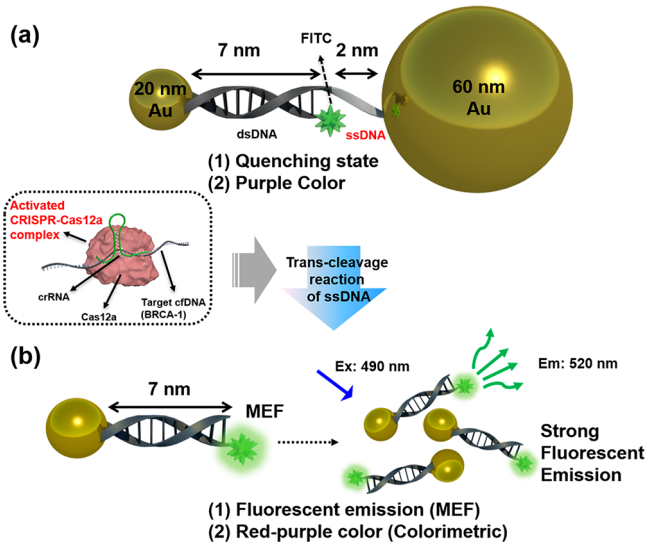

Figure 1. Schematic diagram illustrating our proposed cell-free DNA (cfDNA) detection method using DNA-functionalized Au nanoparticles via colorimetric and metal enhanced fluorescence (MEF). (a) A 20 nm sized Au nanoparticle (20-AuNP) and 60 nm sized Au nanoparticle (60-AuNP) connected by a FITC-modified double-strand DNA (dsDNA) and single-strand DNA (ssDNA); the color of this complex was purple and fluorescent emission was quenched. (b) CRISPR-Cas12a activation via complementary binding of crRNA and target cfDNA (BRCA-1) degrades the ssDNA between 20- and 60-AuNPs via the trans-cleavage effect, after which FITC emitted a strong fluorescence signal at 520 nm.

strong fluorescent quencher when the distance between 60-AuNP and FITC was approximately below 2 nm. The complementarily bound DNA complex was composed of two parts, one of which was the double-strand region, which maintained the optimal distance between 20-AuNPs and FITC to induce MEF; the other was a single-strand region, which maintained the quenching distance and could be cleaved by the activated CRISPR-Cas12a complex. Given that the activated CRISPR-Cas12a complex could only cut the ssDNA and not the dsDNA, the change of the fluorescence intensity signal was expected to be drastic between the inactivated and activated CRISPR-Cas12a complex. Moreover, changes in the distance between 20- and 60-AuNPs led to the alteration of their optical properties, as demonstrated by absorbance peak shifts and color changes. During their nonreaction state (Figure 1a), the color of the AuNP complex was purple, which was different from the unfunctionalized 20-AuNP and 60-AuNPs (red-purple). When the activated CRISPR-Cas12a complex degraded the short ssDNA bridge, their color returned to the original red-purple tone (Figure 1b). Therefore, we could easily verify the presence of target DNA with the naked eye, as well as through a highly sensitive assay based on fluorescence signal changes via the MEF effect. Notably, this fluorescence signal enhancement strategy enabled the elimination of nucleic acid amplification steps, including RPA and LAMP, while still possessing a femtomolar detection limit range. Therefore, this novel nanosensor could overcome the many limitations of conventional amplification-based approaches such as time-consuming reactions, high costs, false-positive signals, complex primer design, and complex optimization steps, all while maintaining high target specificity and sensitivity. Transmission electron microscope (TEM) analyses were conducted to verify ssDNA functionalization on each AuNPs. Specifically, functionalization was confirmed by

https://dx.doi.org/10.1021/acs.nanolett.0c04303
Nano Lett. XXXX, XXX, XXX−XXX

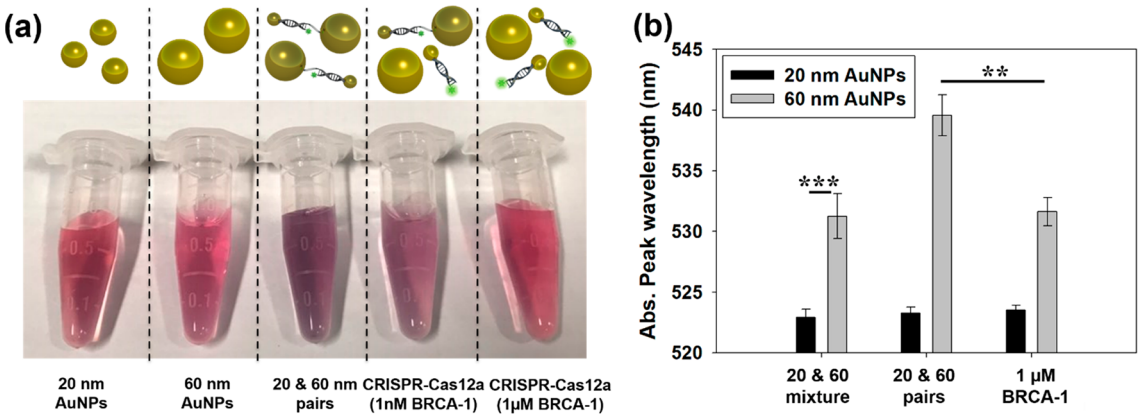

Figure 2. CRISPR-Cas12a-assisted cfDNA detection via color changes of AuNPs. (a) Schematics representing the several color changes of AuNPs depending on assay conditions (20-AuNP, 60-AuNP, DNA-functionalized 20- and 60-AuNP, 20- and 60-AuNP with CRISPR-Cas12a activated by 1 nM BRCA-1, and 20- and 60-AuNP with CRISPR-Cas12a activated by 1 μM BRCA-1, respectively). (b) Peak intensities of the DNA-functionalized 20- and 60-AuNPs before and after the CRISPR-Cas12a activation reaction. Peak intensities were expressed as mean ± SEM ($n = 5$). $^{**}p < 0.001$, $^{***}p < 0.0001$, Student's unpaired t test.

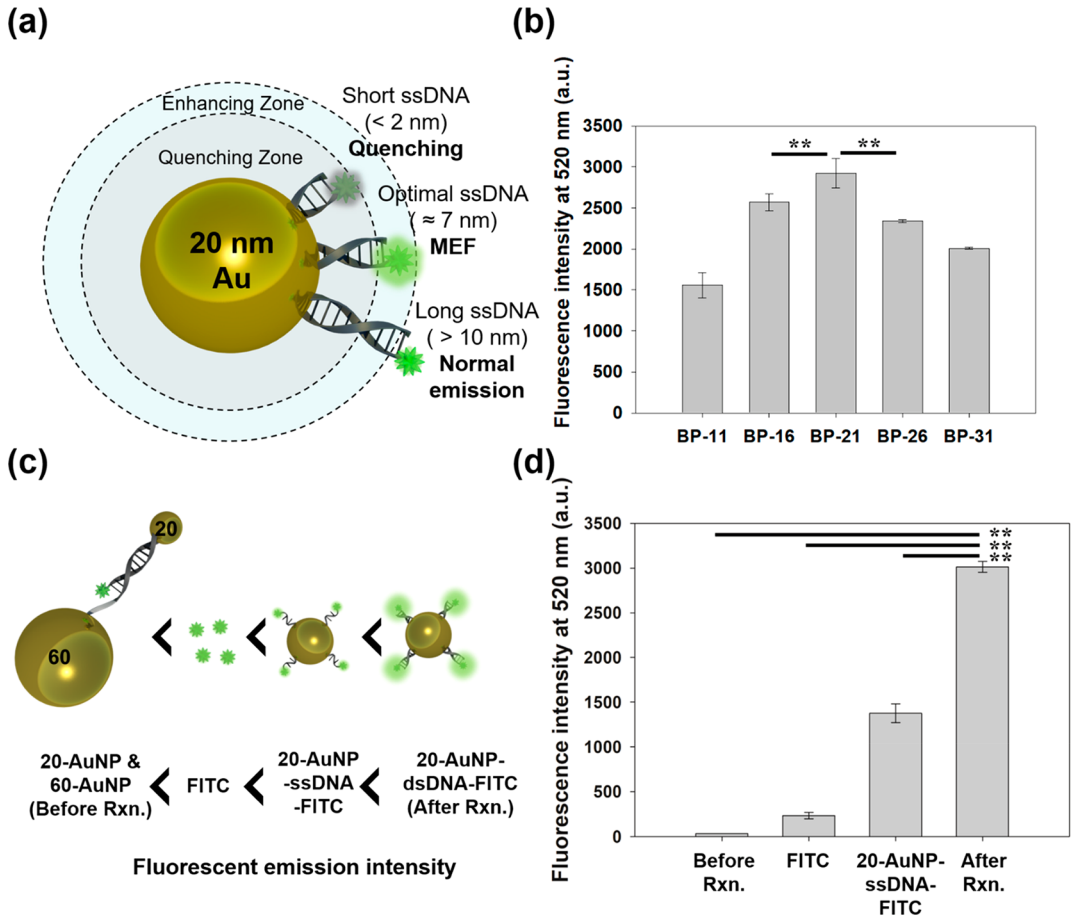

Figure 3. MEF effect of the DNA-functionalized 20- and 60-AuNPs. (a) Schematic diagram of the MEF effect dependent on the DNA length of dsDNA between 20-AuNPs and FITC. (b) Fluorescence intensities of the 20-AuNP with several lengths of dsDNAs; base-pair (bp) numbers ranged from 11 to 31. Fluorescence intensities were expressed as mean ± SEM ($n = 10$). $^{**}p < 0.001$, Student's unpaired t test. (c) Schematic of fluorescence intensity comparisons, which depended on the quenching and MEF effect on the 20-AuNP. (d) Fluorescence intensities of DNA-functionalized 20- and 60-AuNPs, FITC, ssDNA functionalized 20-AuNPs, and dsDNA-functionalized 20-AuNPs via activated CRISPR-Cas12a, respectively. Fluorescence intensities were expressed as mean ± SEM ($n = 10$). $^{**}p < 0.001$, Student's unpaired t test.

observing the corona layers surrounding the 20- and 60-AuNPs (SI Figure 1).

Colorimetric Analysis of cfDNA by the Activated CRISPR-Cas12a Complex. DNA-functionalized 20- and 60-AuNPs were found to be combined, and their color changed from red-purple to purple due to the surface plasmon effect of AuNPs (Figure 2a). If the distance was too short, AuNPs exhibited plasmonic effects similar to those of aggregates or

https://dx.doi.org/10.1021/acs.nanolett.0c04303
Nano Lett. XXXX, XXX, XXX−XXX

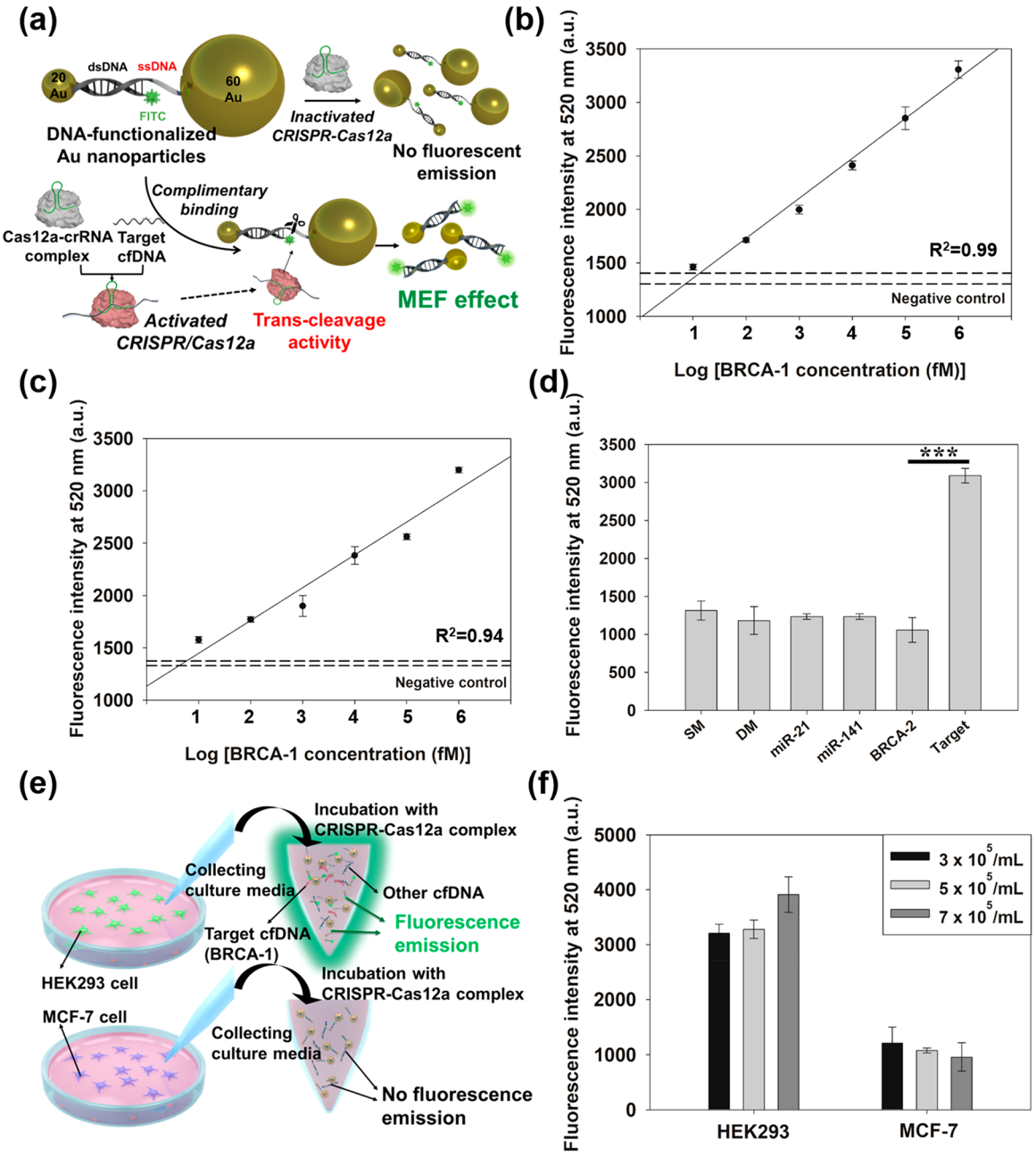

Figure 4. Quantitative and selective cfDNA measurements in buffer solution and human serum. (a) Schematic diagram of CRISPR-Cas12a-mediated sensitive target cfDNA measurement via MEF without nucleic acid amplification. A BRCA-1 sequence activated the CRISPR-Cas12a complex and degraded the ssDNA between the 20- and 60-AuNPs via the trans-cleavage (collateral effect) effect. dsDNA-functionalized 20-AuNP separated from 60-AuNP showed enhanced fluorescence intensity. (b) Fluorescence intensities of Au nanosensor with activated CRISPR-Cas12a for the quantitative measurement of cfDNA ranging from 1 fM to 100 pM concentrations in 20 mM HEPES buffer. Data were expressed as mean ± SEM (n = 10). (c) Fluorescence intensity of the Au nanosensor with activated CRISPR-Cas12a for the quantitative measurement of cfDNA ranging from 1 fM to 100 pM concentrations in 5% human serum. Data intensities were expressed as mean ± SEM (n = 10). (d) Comparison of the fluorescence intensities with different nucleic acids (single-mismatched (SM), double-mismatched (DM), miR-21, miR-141, and BRCA-1 target DNA) for the verification of selective detection. Data are expressed as mean ± SEM (n = 5). ***$p < 0.0001$, Student's unpaired t test. (e) Schematic diagram of the measurement of cfDNA from cell culture media. HEK293 is BRCA-1-positive cell line, which could induce the MEF effect on Au nanosensor, and MCF-7 is BRCA-1-negative cell line. (f) Fluorescence intensity of Au nanosensor with activated CRISPR-Cas12a in HEK293 and MCF-7 culture media from different cell number for the comparative measurement of cfDNA. Fluorescence intensities were expressed as mean ± SEM (n = 5).

larger-sized AuNPs, which present a red-shifted absorbance peak with color changes from red to purple. As expected, the 20-and 60-AuNP binding complex, whose molar ratio is about 20 to 1 before binding reaction, exhibited a characteristic purple color, whereas separate 20- and 60-AuNPs exhibited a red-purple color. On the basis of these observations, the color could be reverted by the dissociation of AuNP, which could be induced by ssDNA degradation between the AuNPs. Applying an activated CRISPR-Cas12a complex (target DNA binding CRISPR-Cas12a complex) to the 20- and 60-AuNP binding complex, a color change was clearly observed. Moreover, in Figure 2a the target DNA concentration (between 1 nM and 1 μM) could be

https://dx.doi.org/10.1021/acs.nanolett.0c04303
Nano Lett. XXXX, XXX, XXX−XXX

differentiated by color changes. This phenomenon could be verified through the change of UV/vis absorbance peaks more precisely (Figure 2b and SI Figure 2). The 20- and 60-AuNPs exhibited absorbance peaks at 523 and 531 nm, respectively. After combining the nanoparticle complex via DNA complementary binding, the absorbance peak of 60-AuNP was shifted to a longer wavelength (approximately 540 nm), whereas the specific absorbance peak of 20-AuNPs remained unchanged due to the remaining unreacted 20-AuNPs to 60-AuNPs. After treating the CRISPR-Cas12a complex with 1 μM of target DNA for 30 min, the absorbance peaks shifted to levels similar to those before the complementary reaction. This result indicated that color and absorbance peak changes depended on the trans-cleavage reaction of the CRISPR-Cas12a by the target DNA. The combined and dissociated AuNPs pairs are also characterized via TEM (SI Figure 3). In SI Figure 3a, some 20-AuNPs were found to wrap around the 60-AuNPs. After CRISPR-Cas12a was treated with 1 nM target DNA, the number of 20-AuNPs pairs wrapped around 60-AuNPs was substantially reduced (SI Figure 3b). This result also supports that conformational changes of AuNPs could be induced by the CRISPR-Cas12a-based trans-cleavage reaction, which could be confirmed by both the change of absorbance peak and naked eye through the color change of the AuNPs pairs.

Verification of MEF Effect on DNA-Functionalized AuNPs for Sensitive cfDNA Detection. To improve the sensitivity of the CRISPR-Cas12a based fluorescent biosensor, the MEF effect was applied to enhance the signal derived from cfDNA measurement via the CRISPR-Cas12a reaction. Notably, the distance between NMNs (i.e., AuNP) and the fluorophore (i.e., FITC) is one of the most critical factors to maximize fluorescence. As mentioned before, if the distance were below 2 nm, the fluorophore would be quenched by the strong effect of the AuNP; however, fluorescence intensity could be maximized at a distance of approximately 7−8 nm. The distance for the induction of MEF could be optimized by adjusting the length of the dsDNA on the 20-AuNPs (Figure 3a). Various dsDNA lengths between the 20-AuNP and FITC were tested, and their fluorescence intensities were measured at 520 nm, which is the emission wavelength of FITC, as well as the absorbance peak of 20-AuNPs. This overlaid specific wavelength at approximately 520 nm is crucial for the induction of the MEF effect, which is closely related to the surface plasmon resonance effect on NMNs. In Figure 3b, 21-base-pair (bp) dsDNA showed the strongest fluorescence enhancing effect, which corresponded with the estimated optimal distance to maximize MEF (approximately 7.14 nm, that is, 0.34 nm per bp). Using this optimal DNA length, changes in fluorescence intensities were observed before and after the target cfDNA binding reaction for the induction of the CRISPR-Cas12a complex trans-cleavage effect (Figure 3c and d). Upon comparing the FITC fluorescence intensities, the 20-AuNP-ssDNA-FITC complex exhibited stronger fluorescence intensity due to the MEF effect. After forming a 20-AuNP and 60-AuNP complex by complementary binding, fluorescence intensity was significantly reduced by the strong quenching effect on 60-AuNPs. Activated CRISPR-Cas12a by the target cfDNA was expected to randomly cleave the ssDNA, thereby regenerating the MEF effect of the 20-AuNP-dsDNA-FITC complex. Interestingly, the CRISPR-Cas12a-assisted reaction provided more enhancing effects than those of 20-AuNP-ssDNA-FITC complexation itself. We anticipated that the dsDNA between the 20-AuNPs and FITC after the CRISPR-Cas12a reaction could help maintain an optimal distance than that of ssDNA. This more than two-fold difference of fluorescence intensities between dsDNA and ssDNA of 20-AuNP and FITC complex could improve the sensitivity of the MEF-based biosensing system. For the comparison of sensitivity in the AuNP-assisted biosensing system using normal fluorescence and MEF effect, cfDNA was measured by using CRISPR-Cas12a-assisted Au nanosensor without MEF effect (SI Figure 4). This non-MEF Au nanosensor, consisting of 20 nm AuNP with thiolated FITC-ssDNA, could show the quenching−dequenching effect. However, using this sensing system exhibited no difference in fluorescence signals to a negative control, ranging from femtomolar to picomolar level of cfDNA.

For the confirmation of ssDNA cleavage by the activated CRISPR-Cas12a complex, we conducted an electrophoresis study (SI Figure 5). ssDNAs, including target DNA and random ssDNA, degraded into small fragments and therefore did not appear as clear lines in the gel. On the other hand, random dsDNA could not be degraded by the activated CRISPR-Cas12a. These observations confirmed that the developed biosensing system exhibited a strong fluorescence signal if the ssDNA between 20-AuNP and 60-AuNP was degraded by the trans-cleavage reaction. This was because the ssDNAs that induced quenching were cleaved, whereas dsDNAs that led to the MEF effect were not degraded. The trans-cleavage reaction by activated CRISPR-Cas12a could also be confirmed by observing the color of the supernatant after the centrifugation at 8000 rpm for 10 min (SI Figure 6). Before the CRISPR-Cas12a reaction on 20−60 AuNPs pairs, they were spun down by centrifugation. However, after the CRISPR-Cas12a reaction, dissociated 20 nm AuNPs from 60 nm AuNPs did not sink down at 8000 rpm and showed red-color in the supernatant. This could also be confirmed by the absorbance peak of the supernatant.

Ultrasensitive Detection of cfDNA by the CRISPR-Cas12a-Assisted MEF Effect on DNA-Functionalized AuNPs. Once the fluorescent signal intensity of 20-AuNP-dsDNA-FITC complex was maximized by an optimal distance (approximately 7 nm), fluorescence intensities were measured with different target concentrations ranging from 1 fM to 100 pM to identify BRCA-1, a representative cfDNA biomarker closely related to breast cancer (Figure 4a). Fluorescence intensity was highly proportional to the BRCA-1 concentration with a high R_2 value of 0.99 (Figure 4b and SI Figure 7). Notably, few-femtomolar concentrations of target DNA could be measured by the CRISPR-Cas12a-assisted AuNP nanosensor system without the need for any target amplification methods. Some published studies using CRISPR-Cas12a as an effector of enzymatic cleavage showed that nucleic acid amplification processes should be integrated into their sensing system to improve sensitivity, thereby reaching a limit of detection (LOD) within the attomolar level. In addition, target recognition of Cas9 and Cas13 proteins to target DNA needs the corresponding protospacer adjacent motif (PAM) sequence. In contrast, using Cas12a as an endonuclease enzyme, activated CRISPR-Cas12a complex exhibited the trans-cleavage effect without the PAM sequence for the ssDNA detection. Therefore, our proposed CRISPR-Cas12a-based sensing system exhibited a femtomolar level LOD without the need for amplification and PAM sequence. The endonuclease property of the CRISPR-Cas12a without PAM showed similar enzymatic activity. For the sensitive detection of cfDNA, we hypothesized that functionalized nanoparticles could enhance the sensing signal and

https://dx.doi.org/10.1021/acs.nanolett.0c04303
Nano Lett. XXXX, XXX, XXX−XXX

improve sensitivity because of their inherent properties, including high surface-to-volume ratio, high reactivity, and providing a highly concentrated substrate (ssDNA) on the AuNPs surface for enzymatic reactions. Moreover, NMNs have superior properties that enhance the fluorescent signals from their inherent SPR effect, thereby simultaneously facilitating the induction of fluorescence quenching and MEF given the appropriate conditions. As a result, ultrasensitive detection of BRCA-1 was successfully achieved through a simple and straightforward method within 30 min, ranging from 1 fM to 100 pM (LOD was obtained as 0.34 fM through the 3.3 × standard deviation of intercept/slope). In the case of a higher level of cfDNA, ranging from 1 to 100 nM, fluorescence signal intensities were saturated (SI Figure 8). As a result, this higher level of cfDNA could not be measured by MEF-based detection, whereas colorimetric methods could cover the nanomolar level of the target cfDNA (SI Figure 2). This simple nanosensor could be applied in simulated physiological conditions using 5% human serum instead of buffer solution, demonstrating a similar target DNA measurement performance (Figure 4c). Regarding specificity, six different ssDNAs, including BRCA-1, were tested. Thr BRCA-1 exhibited significant fluorescence intensity, whereas nontarget DNAs exhibited similar intensities to the negative signal (Figure 4d). The CRISPR-Cas12a complex could only be activated when a specific target DNA was bound to the complementary crRNA. Therefore, the MEF effect could only occur when the CRISPR-Cas12a complex was activated by the target DNA followed by ssDNA cleavage between the 20- and 60-AuNPs.

Because the cfDNA was typically exocytosis from cells, releasing the level of cfDNA could be different according to the origin and status of the cells. In this point of view, BRCA-1 was measured in two other cell culture media from each different cancer cells, which were MCF-7 derived from breast cancer and HEK293 derived from the embryonic kidney (Figure 4e). BRCA-1 has been generally known to express in breast cancers as a mutated form while expressed in other cells. In Figure 4f, BRCA-1 was successfully measured from the HEK293-cultured media in diverse cell numbers. On the other hand, the fluorescence signal was very low in the MCF-7-cultured media, similar to the negative control. This in vitro detection using cell culture media showed the possibility of the nondestructive and noninvasive measurement of cfDNA for the diagnosis of diverse cancers and genetic diseases.

CONCLUSION

In conclusion, cfDNA was sensitively (as low as 0.34 fM) and rapidly (<30 min) detected by using the developed CRISPR-Cas12a-assisted AuNP nanosensor without any amplification method. Compared to other CRISPR-Cas-based detection systems, our developed method overcame the inherent limitations of amplification-based approaches such as being time-consuming, costly, and producing false-positive signals. In our developed system, target amplification was successfully replaced with a signal enhancement strategy via DNA-functionalized AuNP-based MEF. Not only did our proposed method show excellent fluorescence enhancement mediated by the activated CRISPR-Cas12a complex coupled with target DNA, but it also provided the ability to intuitively assess target DNA concentrations via visual inspection of color change. This color change effect could sense target DNA concentration differences down to the nanomolar range, and MEF enabled the measurement of low-level target concentrations ranging from 1 fM to 100 pM. This dual detection system could provide a vast complementary detection range. Moving forward, it is important to explore the potential applications of our developed CRISPR-Cas12a nanosensor for the detection of various DNA targets such as other cfDNAs, genomic DNA, and viral DNA, thereby taking advantage of the inherent specificity of the CRISPR-Cas system. Broadly, our nanosensor may pave new roads for the detection of several diseases in a field-deployable and point-of-care testing platform.

ASSOCIATED CONTENT

Supporting Information

The Supporting Information is available free of charge at https://pubs.acs.org/doi/10.1021/acs.nanolett.0c04303.

Preparation of DNA-functionalized 20- and 60-AuNP, TEM analysis for the confirmation of functionalization and binding formation of 20- and 60-AuNP, colorimetric analysis of target-mediated CRISPR-Cas12a reaction, BRCA-1 detection using MEF-based fluorescence measurements, Materials and Methods, Supplementary Figures 1−8 (PDF)

AUTHOR INFORMATION

Corresponding Authors

Se-Hwan Paek − *SOL Bio Corporation, Seoul 04780, Republic of Korea*; Email: shpaek@korea.ac.kr

Jeong-Woo Choi − *Department of Chemical and Biomolecular Engineering, Sogang University, Seoul 04107, Republic of Korea*; orcid.org/0000-0003-0100-0582; Email: jwchoi@sogang.ac.kr

Authors

Jin-Ha Choi − *Department of Chemical and Biomolecular Engineering, Sogang University, Seoul 04107, Republic of Korea*; orcid.org/0000-0002-1632-9586

Joungpyo Lim − *Department of Chemical and Biomolecular Engineering, Sogang University, Seoul 04107, Republic of Korea*

Minkyu Shin − *Department of Chemical and Biomolecular Engineering, Sogang University, Seoul 04107, Republic of Korea*

Complete contact information is available at: https://pubs.acs.org/10.1021/acs.nanolett.0c04303

Author Contributions

§J.-H.C. and J.L. contributed equally to this work.

Author Contributions

J.-H.C. and J.-W.C. designed the original idea. J.-H.C. conducted the experiments. J.-H.C., J.L., and M.S. wrote the manuscript. S.-H.P. arranged the research fund for this study. S.-H.P. supervised the revising and updating process in this study.

Notes

The authors declare no competing financial interest.

ACKNOWLEDGMENTS

This research was supported by the SOL Bio Corporation.

ABBREVIATIONS

MEF, metal-enhanced fluorescence; AuNP, Au nanoparticle; cfDNA, cell-free DNA; CRISPR, clustered regularly interspaced short palindromic repeats; POCT, point-of-care testing; SERS,

https://dx.doi.org/10.1021/acs.nanolett.0c04303
Nano Lett. XXXX, XXX, XXX−XXX

surface-enhanced Raman spectroscopy; LOD, limit of detection; BRCA-1, breast cancer gene-1; crRNA, CRISPR RNA; tracrRNA, trans-activating CRISPR RNA; LAMP, loop-mediated isothermal amplification; RPA, recombinase polymerase amplification; HPV, human papillomavirus; NMNs, noble metal nanomaterials; dsDNA, double-strand DNA; ssDNA, single-strand DNA; FITC, fluorescein isothiocyanate; TEM, transmission electron microscope; SPR, surface plasmon resonance; bp, base-pair; SM, single-mismatched; DM, double-mismatched

REFERENCES

(1) Cong, L.; Ran, F. A.; Cox, D.; Lin, S. L.; Barretto, R.; Habib, N.; Hsu, P. D.; Wu, X. B.; Jiang, W. Y.; Marraffini, L. A.; Zhang, F. Multiplex Genome Engineering Using CRISPR/Cas Systems. *Science* **2013**, *339*, 819−823.

(2) Faure, G.; Shmakov, S. A.; Yan, W. X.; Cheng, D. R.; Scott, D. A.; Peters, J. E.; Makarova, K. S.; Koonin, E. V. CRISPR-Cas in mobile genetic elements: counter-defence and beyond. *Nat. Rev. Microbiol.* **2019**, *17*, 513−525.

(3) Hsu, P. D.; Lander, E. S.; Zhang, F. Development and applications of CRISPR-Cas9 for genome engineering. *Cell* **2014**, *157*, 1262−1278.

(4) McCarty, N. S.; Graham, A. E.; Studena, L.; Ledesma-Amaro, R. Multiplexed CRISPR technologies for gene editing and transcriptional regulation. *Nat. Commun.* **2020**, *11*, 1281.

(5) Cheng, Q.; Wei, T.; Farbiak, L.; Johnson, L. T.; Dilliard, S. A.; Siegwart, D. J. Selective organ targeting (SORT) nanoparticles for tissue-specific mRNA delivery and CRISPR-Cas gene editing. *Nat. Nanotechnol.* **2020**, *15*, 313−320.

(6) Eyquem, J.; Mansilla-Soto, J.; Giavridis, T.; van der Stegen, S. J.; Hamieh, M.; Cunanan, K. M.; Odak, A.; Gonen, M.; Sadelain, M. Targeting a CAR to the TRAC locus with CRISPR/Cas9 enhances tumour rejection. *Nature* **2017**, *543*, 113−117.

(7) He, X. Y.; Ren, X. H.; Peng, Y.; Zhang, J. P.; Ai, S. L.; Liu, B. Y.; Xu, C.; Cheng, S. X. Aptamer/Peptide-Functionalized Genome-Editing System for Effective Immune Restoration through Reversal of PD-L1-Mediated Cancer Immunosuppression. *Adv. Mater.* **2020**, *32*, 2000208.

(8) Liu, C.; Zhang, L.; Liu, H.; Cheng, K. Delivery strategies of the CRISPR-Cas9 gene-editing system for therapeutic applications. *J. Controlled Release* **2017**, *266*, 17−26.

(9) Picco, G.; Chen, E. D.; Alonso, L. G.; Behan, F. M.; Gonçalves, E.; Bignell, G.; Matchan, A.; Fu, B.; Banerjee, R.; Anderson, E. Functional linkage of gene fusions to cancer cell fitness assessed by pharmacological and CRISPR-Cas9 screening. *Nat. Commun.* **2019**, *10*, 1−12.

(10) Wang, P.; Zhang, L.; Xie, Y.; Wang, N.; Tang, R.; Zheng, W.; Jiang, X. Genome Editing for Cancer Therapy: Delivery of Cas9 Protein/sgRNA Plasmid via a Gold Nanocluster/Lipid Core-Shell Nanocarrier. *Adv. Sci.* **2017**, *4*, 1700175.

(11) Wang, T.; Liu, Y.; Sun, H. H.; Yin, B. C.; Ye, B. C. An RNA-Guided Cas9 Nickase-Based Method for Universal Isothermal DNA Amplification. *Angew. Chem., Int. Ed.* **2019**, *58*, 5382−5386.

(12) Wang, X.; Xiong, E.; Tian, T.; Cheng, M.; Lin, W.; Wang, H.; Zhang, G.; Sun, J.; Zhou, X. Clustered Regularly Interspaced Short Palindromic Repeats/Cas9-Mediated Lateral Flow Nucleic Acid Assay. *ACS Nano* **2020**, *14*, 2497−2508.

(13) Young, C. S.; Hicks, M. R.; Ermolova, N. V.; Nakano, H.; Jan, M.; Younesi, S.; Karumbayaram, S.; Kumagai-Cresse, C.; Wang, D.; Zack, J. A.; Kohn, D. B.; Nakano, A.; Nelson, S. F.; Miceli, M. C.; Spencer, M. J.; Pyle, A. D. A Single CRISPR-Cas9 Deletion Strategy that Targets the Majority of DMD Patients Restores Dystrophin Function in hiPSC-Derived Muscle Cells. *Cell stem cell* **2016**, *18*, 533−40.

(14) Zhou, W.; Hu, L.; Ying, L.; Zhao, Z.; Chu, P. K.; Yu, X. F. A CRISPR-Cas9-triggered strand displacement amplification method for ultrasensitive DNA detection. *Nat. Commun.* **2018**, *9*, 5012.

(15) Yan, W. X.; Hunnewell, P.; Alfonse, L. E.; Carte, J. M.; Keston-Smith, E.; Sothiselvam, S.; Garrity, A. J.; Chong, S.; Makarova, K. S.; Koonin, E. V.; Cheng, D. R.; Scott, D. A. Functionally diverse type V CRISPR-Cas systems. *Science* **2019**, *363*, 88−91.

(16) Li, S.-Y.; Cheng, Q.-X.; Wang, J.-M.; Li, X.-Y.; Zhang, Z.-L.; Gao, S.; Cao, R.-B.; Zhao, G.-P.; Wang, J. CRISPR-Cas12a-assisted nucleic acid detection. *Cell discov.* **2018**, *4*, 1−4.

(17) Pickar-Oliver, A.; Gersbach, C. A. The next generation of CRISPR-Cas technologies and applications. *Nat. Rev. Mol. Cell Biol.* **2019**, *20*, 490−507.

(18) Chen, J. S.; Ma, E.; Harrington, L. B.; Da Costa, M.; Tian, X.; Palefsky, J. M.; Doudna, J. A. CRISPR-Cas12a target binding unleashes indiscriminate single-stranded DNase activity. *Science* **2018**, *360*, 436−439.

(19) Mukama, O.; Wu, J.; Li, Z.; Liang, Q.; Yi, Z.; Lu, X.; Liu, Y.; Liu, Y.; Hussain, M.; Makafe, G. G.; Liu, J.; Xu, N.; Zeng, L. An ultrasensitive and specific point-of-care CRISPR/Cas12 based lateral flow biosensor for the rapid detection of nucleic acids. *Biosens. Bioelectron.* **2020**, *159*, 112143.

(20) Wang, B.; Wang, R.; Wang, D.; Wu, J.; Li, J.; Wang, J.; Liu, H.; Wang, Y. Cas12aVDet: A CRISPR/Cas12a-Based Platform for Rapid and Visual Nucleic Acid Detection. *Anal. Chem.* **2019**, *91*, 12156−12161.

(21) Wu, H.; Qian, C.; Wu, C.; Wang, Z.; Wang, D.; Ye, Z.; Ping, J.; Wu, J.; Ji, F. End-point dual specific detection of nucleic acids using CRISPR/Cas12a based portable biosensor. *Biosens. Bioelectron.* **2020**, *157*, 112153.

(22) Volik, S.; Alcaide, M.; Morin, R. D.; Collins, C. Cell-free DNA (cfDNA): Clinical Significance and Utility in Cancer Shaped by Emerging Technologies. *Mol. Cancer Res.* **2016**, *14*, 898−908.

(23) Kahlert, C. Liquid Biopsy: Is There an Advantage to Analyzing Circulating Exosomal DNA Compared to cfDNA or Are They the Same? *Cancer Res.* **2019**, *79*, 2462−2465.

(24) Chen, Y.; Munechika, K.; Ginger, D. S. Dependence of fluorescence intensity on the spectral overlap between fluorophores and plasmon resonant single silver nanoparticles. *Nano Lett.* **2007**, *7*, 690−696.

(25) Li, M.; Cushing, S. K.; Wu, N. Plasmon-enhanced optical sensors: a review. *Analyst* **2015**, *140*, 386−406.

(26) Choi, J. H.; El-Said, W. A.; Choi, J.-W. Highly sensitive surface-enhanced Raman spectroscopy (SERS) platform using core/double shell (Ag/polymer/Ag) nanohorn for proteolytic biosensor. *Appl. Surf. Sci.* **2020**, *506*, 144669.

(27) Kim, T. H.; Lee, K. B.; Choi, J. W. 3D graphene oxide-encapsulated gold nanoparticles to detect neural stem cell differentiation. *Biomaterials* **2013**, *34*, 8660−8670.

(28) Lee, J. H.; Choi, J. H.; Chueng, S. D.; Pongkulapa, T.; Yang, L.; Cho, H. Y.; Choi, J. W.; Lee, K. B. Nondestructive Characterization of Stem Cell Neurogenesis by a Magneto-Plasmonic Nanomaterial-Based Exosomal miRNA Detection. *ACS Nano* **2019**, *13*, 8793−8803.

(29) Ribeiro, T.; Baleizao, C.; Farinha, J. P. S. Artefact-free Evaluation of Metal Enhanced Fluorescence in Silica Coated Gold Nanoparticles. *Sci. Rep.* **2017**, *7*, 2440.

(30) Wang, K.; Dong, Y. H.; Li, B. Y.; Li, D. Y.; Zhang, S. C.; Wu, Y. Y. Differentiation of proteins and cancer cells using metal oxide and metal nanoparticles-quantum dots sensor array. *Sens. Actuators, B* **2017**, *250*, 69−75.

(31) Choi, J. H.; Choi, J. W. Metal-enhanced fluorescence by bifunctional Au nanoparticles for highly sensitive and simple detection of proteolytic enzyme. *Nano Lett.* **2020**, *20*, 7100−7107.

https://dx.doi.org/10.1021/acs.nanolett.0c04303
Nano Lett. XXXX, XXX, XXX−XXX